 doi:10.20944/preprints202108.0477.v1

Article

Experimental Investigation into the Effect of Surface Roughness and Mechanical Properties of 3D-Printed Titanium Ti-64 ELI after Heat Treatment

***Lebogang Lebea [1,2], Harry M Ngwangwa [2], Dawood Desai[1] and Fulufhelo Nemavhola[2]**

[1] Department of Mechanical and Mechatronic Engineering, Tshwane University of Technology, lebealc@unisa.ac.za
[2] Unisa Biomechanics Research Group, Department of Mechanical and Industrial Engineering, University of South Africa, masitfj@unisa.ac.za

* Correspondence: lebealc@unisa.ac.za

Abstract: The initial stability after implantology is paramount to the survival of the dental implant and the surface roughness of the implant plays a vital role in this regard. The characterisation of surface topography is a complicated branch of metrology, with a huge range of parameters available. Each parameter contributes significantly towards the survival and mechanical properties of 3D-printed specimens. The purpose of this paper is to experimentally investigate the effect of surface roughness of 3D-printed dental implants and 3D-printed dogbone tensile samples under areal height (Ra) parameters, amplitude parameters (average of ordinates), skewness (Rsk) parameters and mechanical properties. During the experiment, roughness values were analysed and the results showed that the skewness parameter demonstrated a minimum value of 0.596%. The 3D-printed dental implant recorded Ra with a 3.4 mm diameter at 43.23% and the 3D-printed dental implant with a 4.3 mm diameter at 26.18%. Samples with a complex geometry exhibited a higher roughness surface, which was the greatest difficulty of additive manufacturing when evaluating surface finish. The results show that when the ultimate tensile stress (UTS) decreases from 968.35 MPa to 955.25 MPa, Ra increases by 1.4% and when UTS increases to 961.18 MPa, Ra increases by 0.6%. When the cycle decreases from 262142 to 137433, Ra shows that less than a 90.74% increase in cycle is obtained. For 3D-printed dental implants, the higher the surface roughness, the lower the mechanical properties, ultimately leading to decreased implant life and poor performance.

Keywords: *3D printing, surface roughness, powder bed fusion*

1. Introduction

The mechanical behaviour of a structure is one of the most important factors to consider in the design of a dental implant [1]. The use of additive manufacturing is a useful tool in the design and production of dental implants [2]; however, despite many attempts this technology is still in the initial research stage [3]. The effect of surface roughness on the final product produced by additive manufacturing still lacks attention, especially when printing complex structures.

Recently, titanium has acquired a position in additive manufacturing technology in the production of dental implants [4]. The production of this material leads to the possibility of using three-dimensional (3D) printing in the field of tissue engineering, which allows for the production of scaffolds with patient-specific dimensions (Becker, Van Rooyen and Dimitrov, 2015; Ren *et al.*, 2021). Regardless of the increased effectiveness of titanium, the capability to produce parts or products with high productivity and superior quality is a challenge [7]. Extra low interstitial (ELI) titanium or Ti-64 ELI is a

 doi:10.20944/preprints202108.0477.v1

well-known light alloy characterised by excellent mechanical properties and corrosion resistance combined with low specific weight and biocompatibility [8]. This material is ideal for many high-performance applications [9].

The use of microscopes is becoming increasingly popular as technology in material characterisation [10]. Surface roughness, which is an unavoidable phenomenon at machining, is usually strictly required when the processed materials are applied in structural components subjected to cyclic loads [11]. Surface roughness is usually characterised by an average geometric parameter, namely arithmetic mean roughness (Ra) [12]. Moreover, the accuracy and efficiency of roughness measurements are important to the modern industry [6]. Surface treatments on titanium materials have been in existence for a long time [13]–[15]; however, technologies involved in this treatment have evolved in the last 10 years [16]. It was reported that surface roughness plays a critical role in determining the life of the implant [17].

The characterisation of surface topography and roughness are imperative in unfolding the wear and damage to surfaces [18]. Surface roughness characterisation and the electron beam melting (EBM) process were analysed, and the authors found that the mean roughness value (Ra) agreed with that of the literature on the EBM process [19]. Recently, five tensile specimen made of TI-64 with different roughness profiles were examined experimentally and the results showed failure of Ti-64 to be highly sensitive to both magnitude and orientation of roughness [20]. Surface roughness and texture can influence the biological response around implants; as such, it is paramount to investigate this phenomenon carefully [21]. Experimental studies have been conducted to determine the surface roughness and morphology of 3D-printed samples [22]–[24]. However, despite many attempts, the performance-based parameters of 3D-printed Ti-64 ELI material is not well established. The aim of this study was to investigate experimentally the effect of 3D-printed dental implants with 3.4 and 4.3 mm diameters and 3D-printed dogbone tensile specimen surface topography and mechanical properties under areal height parameters, amplitude parameters (average of ordinates) and skewness parameter. The outcome of this study can contribute significantly to understanding the variation between various roughness topography of direct metal laser sintering (DMLS) 3D-printed samples.

2. Materials and Methods

The design of dental implants was carried out by the authors at the University of South Africa using Abaqus CAE software and then saved as a .STL file format, which is one of the most common file formats used in 3D printing process. The designed dental implants were of dimeters 3.4 mm and 4.3 mm. TiziriTech (South Africa) was contracted to manufacture the dental implants through direct laser sintering 3D printing technique. The direct metal laser sintering machine (EOS M290) is used for sample preparation on a Titanium Ti-64 ELI powder (specifications listed in Table 1). Before starting the sample building, the build plate is preheated to 40 °C. The average size of the particles was 39±3 μm. The layer thickness was fixed at 20 μm with a volume rate of 1.68 mm^3/s. The total build speed depends on this volume rate and many other factors such as exposure parameters of contours, supports, up and down skin, recoating time, Home-In or LPM settings. The build

Preprints (www.preprints.org) | NOT PEER-REVIEWED | Posted: 24 August 2021 doi:10.20944/preprints202108.0477.v1

job was processed by the EOS DMLS™ system: EOS M290, 63-µm mesh for powder sieving is recommended.

Table 1: Direct metal laser sintering machine (EOS M290) specifications.

Parameter	Values
Laser power	Yb fibre laser: 400 W
Scan speed	Up to 7.0 m/s
Wavelength	1060–1100 mm
Build area	250 × 250 × 325 mm
Diameter of laser beam	100–500 µm

To increase the mechanical properties and burn off excess binder, the heat treatment procedure was performed for 2 hours held at 800 ^{0}C in a protective argon atmosphere. Cooling was done at room temperature in a protective atmosphere to reduce oxidation. The chemical composition of the material is represented in Table 2.

Table 2: Chemical composition of titanium Ti-64 ELI (extra low interstitials) powder in wt. %.

Al	V	O	N	C	H	Fe	Y	Other elements	Ti
6.50	4.50	0.13	0.05	0.08	0.012	0.25	0.005	0.1	bal.

Preprints (www.preprints.org) | NOT PEER-REVIEWED | Posted: 24 August 2021 doi:10.20944/preprints202108.0477.v1

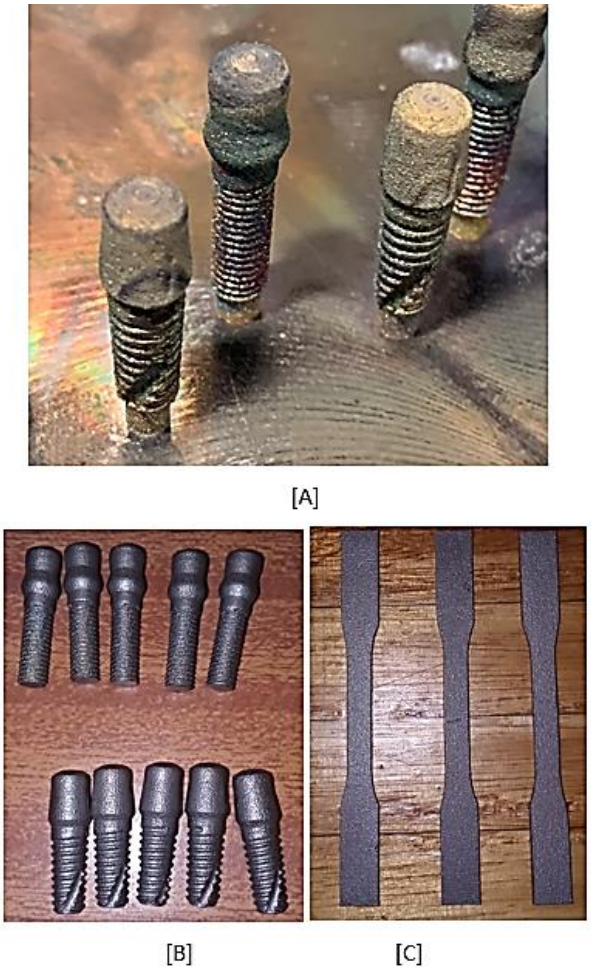

Figure 1: 3D-printed specimens printed with a direct metal laser sintering machine (EOS M290). [A] 3D-printed dental implants before heat treatment, [B] 3D-printed dental implants after heat treatment, [C] 3D-printed dogbone tensile specimen after heat treatment. The heat treatment was performed for 2 hours held at 800 ^{0}C in a protective argon atmosphere.

2.1. Surface roughness measurements after heat treatment

To investigate the effect of performance-based parameters, the specimens were placed in a specimen holder of a confocal microscope ZEISS LSM 900 for materials (see Figure 2). The surface roughness values of samples were measured at a horizontal direction of 3D-printed dental implants with 3.4 and 4.3 mm diameters and 3D-printed dogbone tensile test specimens. The master grain was adjusted until the optimum value was reached and 10 × microscopic laser was selected. Surface roughness measurements were taken from 600 × 600 μm length on each specimen in horizontal direction. Three specimens were selected in each group, namely a 3D-printed dental implant with V-type threads and a 3.4 mm diameter, a 3D-printed dental implant with V-type threads and a 4.5 mm diameter, and a 3D-printed dogbone tensile test specimen. The surface roughness values were determined by calculating the average of these measurements.

Preprints (www.preprints.org) | NOT PEER-REVIEWED | Posted: 24 August 2021 doi:10.20944/preprints202108.0477.v1

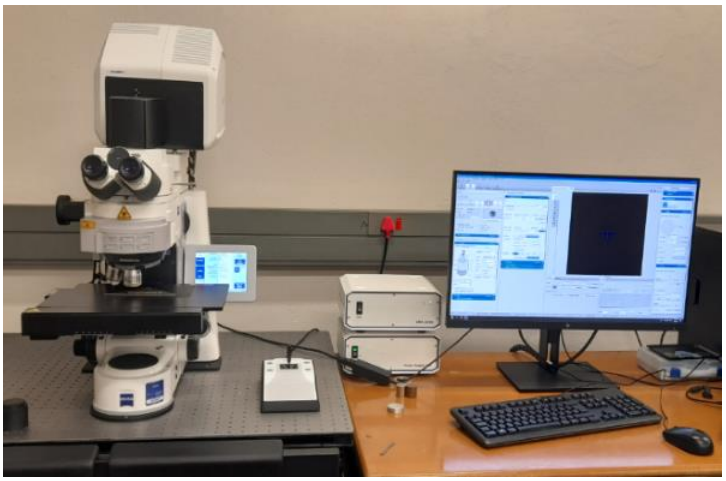

Figure 2: Experimental setup of surface roughness measurement using a confocal microscope ZEISS LSM 900.

The surface topography algorithm is paramount in analysing roughness values. Three algorithms – areal height parameters (R), amplitude parameters (S) and skewness (Rsk) – are used to calculate these parameters [25]. Average roughness is a value that calculates the absolute magnitude of surface features without considering the nature of the surface and skewness is the ratio of the mean of the height values. However, the root mean square roughness value accounts for the size disparity of features, as it presents an average roughness value.

2.2. Tensile test experiment after heat treatment

The dog bone tensile specimens were 3D-printed on an EOS 290 powder bed fusion printer. The specimens were prepared following ASTM standard E8/E8M-09 (standard test methods for the tension testing of metallic material) [26]. The tensile test was performed on a 10 KN Instron electro-mechanical controlled testing machine. The machine was loaded at a crosshead velocity of 3 mm per minute. For statistical considerations, four 3D-printed specimens were tested. The specimens were finally fractured after necking. The maximum force, tensile stress at yield (offset 2%) and ultimate tensile strength (UTS) were recorded; and are presented in Table 1.

2.3. Fatigue test after heat treatment

The physical specimens were tested at a frequency of 10 Hz using an MTS Acumen fatigue machine until fracture occurred. A maximum load of 810.50 N was selected [27]. The specimens were fixed according to the International Standard of dynamic testing of single-post endosseous dental implants [28]. It was reported that under ISO protocol, testing in air and a normal saline solution are equivalent in terms of the likelihood of fracture versus runouts [27]. As such, the current study considered air as a testing environment. Dental implants with a diameter of 3.4 mm were 3D-printed and tested experimentally.

Preprints (www.preprints.org) | NOT PEER-REVIEWED | Posted: 24 August 2021 doi:10.20944/preprints202108.0477.v1

3. Results

To evaluate the results, 18 visual signatures of all the surfaces were compared. The other information (2D roughness measurement profile and roughness graph) was used to aid in the analysis of the coefficient behaviour. The tests were carried out on the samples by selecting 3 equal points on the samples. The experimental results were then displayed in Tables 4 to 6 to calculate the mean, variance and standard deviations. The visual signatures of dogbone 3.4 mm and 4.3 mm dental implants are shown in Figure 3. The graphs are plotted using the mean values of each roughness parameter. The comparison of results obtained at different models indicates which model geometry is sensitive to the printing process according to the desired roughness level.

Tables 3 to 5: Experimental data of 3D-printed dental implants with a diameter of 3.4 mm, 3D-printed dental implants with a diameter of 4.3 mm and 3D-printed dogbone tensile specimen.

Table 3		3.4 mm	Dental implant
1	Mean	Variance	Standard deviation
Ra	5.338	8.008	2.829
Rq	6.728	10.093	3.176
Rsk	0.602	0.904	0.951
Sq	60.533	90.800	9.528
Sa	53.407	80.110	8.950
Ssk	0.253	0.379	0.616
2	Mean	Variance	Standard deviation
Ra	9.943	14.915	3.862
Rq	12.297	18.446	4.294
Rsk	0.573	0.861	0.927
Sq	54.490	81.735	9.041
Sa	46.713	70.070	8.371
Ssk	0.175	0.263	0.512
3	Mean	Variance	Standard deviation
Ra	4.332	6.499	2.549
Rq	5.456	8.185	2.861
Rsk	0.609	0.914	0.956
Sq	40.967	61.450	7.839
Sa	35.843	53.765	7.332
Ssk	0.077	0.116	0.341

Table 4		Tensile	Dogbone
1	Mean	Variance	Standard deviation
Ra	4.094	6.142	2.478
Rq	5.866	8.799	2.966
Rsk	0.796	1.195	1.093
Sq	13.710	20.565	4.534
Sa	10.620	15.931	3.991
Ssk	0.361	0.541	0.7354
2	Mean	Variance	Standard deviation
Ra	4.482	6.723	2.592
Rq	5.967	8.951	2.992
Rsk	0.848	1.273	1.128
Sq	12.107	18.160	4.261
Sa	9.356	14.034	3.746
Ssk	0.301	0.452	0.672
3	Mean	Variance	Standard deviation
Ra	4.537	6.806	2.608
Rq	5.984	8.976	2.995
Rsk	1.107	1.661	1.288
Sq	12.693	19.040	4.363
Sa	9.917	14.876	3.857
Ssk	0.477	0.717	0.847

Preprints (www.preprints.org) | NOT PEER-REVIEWED | Posted: 24 August 2021 doi:10.20944/preprints202108.0477.v1

Table 5	4.3 mm		Dental implant
1	**Mean**	**Variance**	**Standard deviation**
Ra	6.023	9.035	3.006
Rq	8.027	12.041	3.470
Rsk	1.062	1.593	1.262
Sq	52.163	78.245	8.846
Sa	47.730	71.595	8.461
Ssk	0.117	0.176	0.419
2	**Mean**	**Variance**	**Standard deviation**
Ra	5.525	8.288	2.878
Rq	7.145	10.717	3.273
Rsk	0.861	1.292	1.137
Sq	53.573	80.360	8.964
Sa	48.437	72.655	8.524
Ssk	0.250	0.375	0.613
3	**Mean**	**Variance**	**Standard deviation**
Ra	4.582	6.873	2.622
Rq	6.056	9.085	3.014
Rsk	0.879	1.318	1.148
Sq	53.150	79.725	8.928
Sa	47.737	71.605	8.462
Ssk	0.192	0.287	0.536

Preprints (www.preprints.org) | NOT PEER-REVIEWED | Posted: 24 August 2021 doi:10.20944/preprints202108.0477.v1

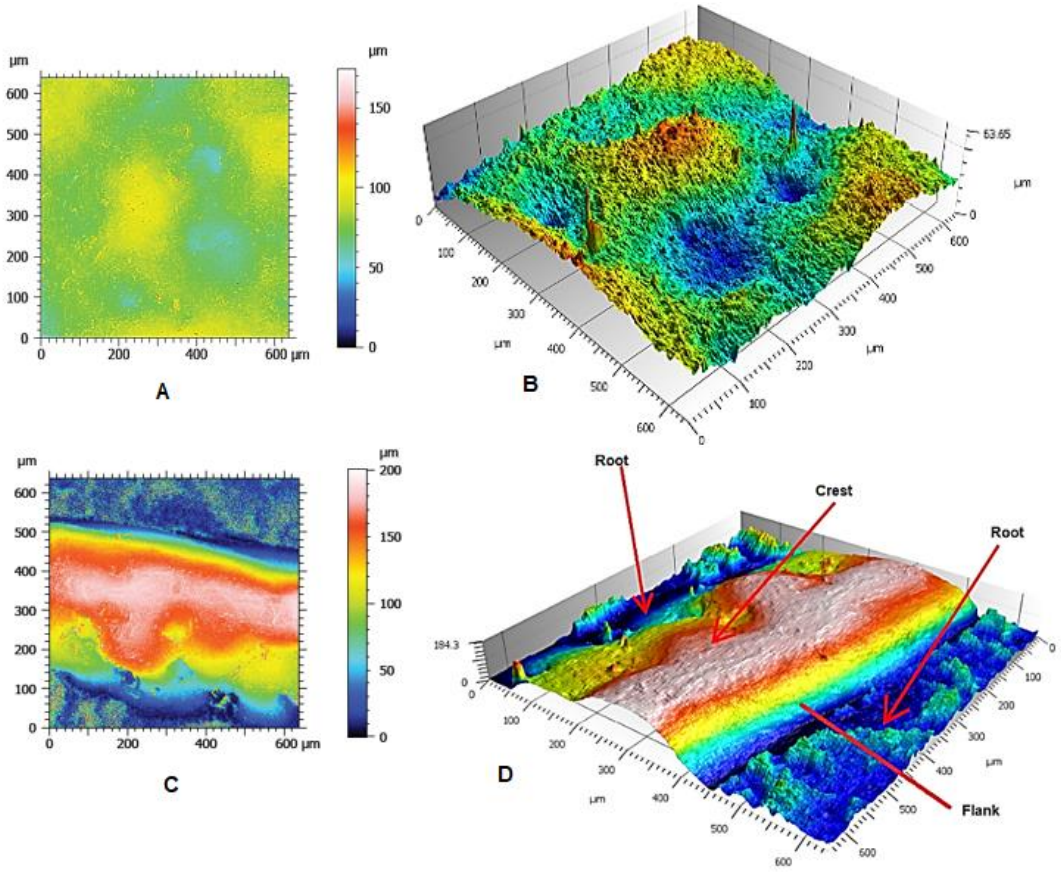

Figure 3: 2D and 3D surface roughness profile of 3D-printed dog bone tensile specimen [see frames A-B], 3D-printed dental implant surface roughness profile 4.3 mm in 2D and 3D views [see frames C–D], 3D-printed dental implant surface roughness profile 3.4 mm in 2D and 3D views [see frames E–F].

3.1. Effect of heat treatment on surface roughness

3.1.1. Arithmetic mean (Ra and Sa)

The underlying surface topography was characterised by measuring the arithmetic mean roughness values. The length of 600 μm was used on the 3D-printed dogbone tensile specimen and 3D-printed dental implants with diameters of 3.4 and 4.3 mm. A length of 600 μm was used for the 3D-printed dogbone tensile specimens and 3D-printed dental implants with diameters of 3.4 and 4.3 mm. Figure 4 compares the curves of the height parameter (Ra) and the amplitude parameter (Sa) of three instances of the magnitude of different nominal roughness of the surface

Preprints (www.preprints.org) | NOT PEER-REVIEWED | Posted: 24 August 2021 doi:10.20944/preprints202108.0477.v1

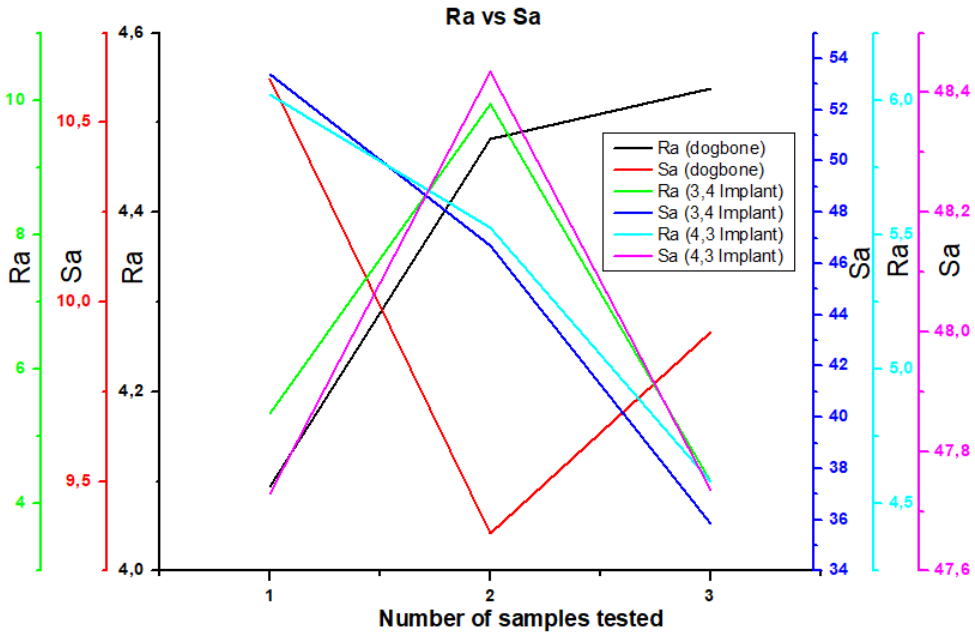

Figure 4: Graphical representation of 3D-printed specimen results with comparison of arithmetic mean roughness (Ra and Sa) μm. A 3D-printed dogbone tensile specimen, 3D-printed dental implant with as 3.4 mm diameter and 3D-printed dental implant with a 4.3 mm diameter are plotted against the number of specimens.

Currently, most studies pay more attention to lower roughness values of < 5 μm, since it is suggested that Ra values of 3 to 5 μm will be more favourable for osteoblast responses than smooth surfaces with Ra values < 1 μm [29]–[31]. In the present study, dental implants and dogbone tensile specimens were fabricated using the DMLS technique. The surface topography of the samples was then analysed using confocal microscopy. The results show that the lowest value of the 3D- printed tensile specimen (Ra) was 4.094 μm and the highest value was 4.537 μm. The minimum roughness value Ra of the 3D-printed dental implant with a diameter of 3.4 mm was 4.333 μm and the maximum Ra was 9.944 μm. The surface roughness (Ra) of 3D-printed dental implants with a diameter of 4.3 mm was reported to be a minimum of 4.582 μm and a maximum of 6.023 μm, which is consistent with previously reported studies [32], [33]. The surface roughness (Ra) results demonstrated significant improvement in 3.4 mm diameter with 43.23% and 4.3 mm diameter implants at 26.18%, compared to previous studies [23], [34].

3.1.2. Root mean square (Rq and Sq)

The root mean square deviation of the surface from the reference plane is evaluated in the Figure 5. Previous studies have shown that the printing orientation has a tremendous effect on the quality of the surface texture and that it is possible to set digital models on the building platform [35]. Deviations between models were recorded, and the Rq value of the 3D-printed dogbone tensile test specimens was 6.94%, the 3D-printed dental implant with a 3.4 mm diameter was 8.16% and the 3D-printed dental implant with a 4.3 mm diameter was 7.076%. Percentages are calculated as the average of each point on

Preprints (www.preprints.org) | NOT PEER-REVIEWED | Posted: 24 August 2021 doi:10.20944/preprints202108.0477.v1

the graph. Based on the experimental data, it was observed that the Rq of 3D-printed dental implants with a diameter of 3.4 mm was higher, which came as no surprise because the geometry of the 3D-printed implant was smaller and complex to build with the additive manufacturing technique. The results of the 3D-printed dogbone tensile test piece in Figure 5 show that Sq is the lowest percentage of 14.77% compared to 3D-printed dental implants with a diameter of 3.4 mm at 52% and 3D-printed dental implants with a diameter of 4.3 mm at 53%. This shows that the 3D-printing process is more effective on improved surfaces when printing flat specimens than complex shapes. The Rq and Sq results compared favourably to previous studies of the surface treatment performance of TI6AI 4V produced by additive manufacturing [36], [37].

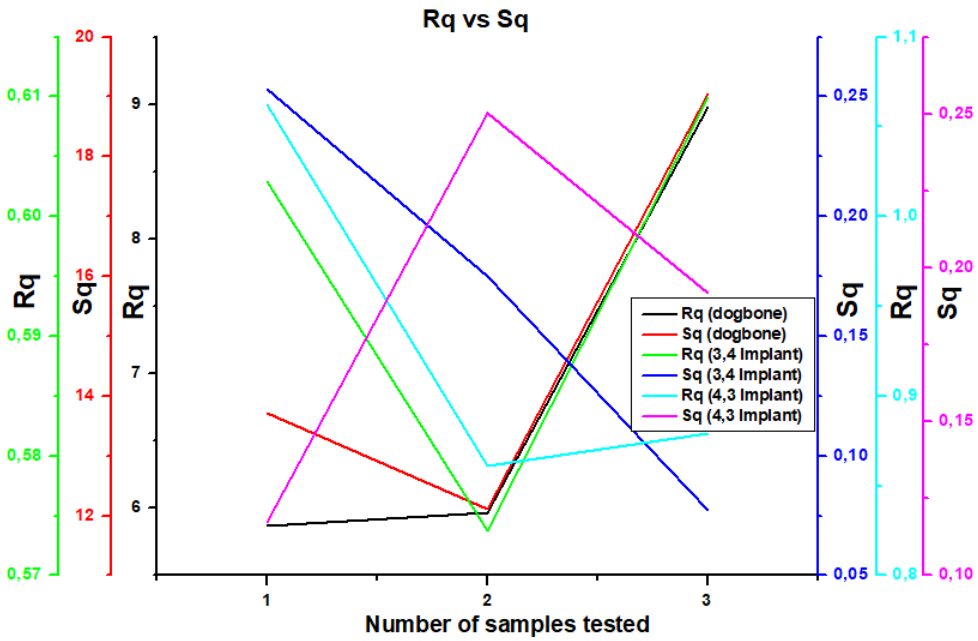

Figure 5: Graphical representation of 3D-printed specimen results with comparison of the root mean square (Rq and Sq) μm. 3D-printed dogbone tensile specimens, 3D-printed dental implant with a 3.4 mm diameter and 3D-printed dental implant with a 4.3 mm diameter are plotted against the number of specimens.

The root mean square (Rq and Sq) parameters are the simplest and most widely used amplitude parameters [7], [35]. In addition to the effective value (Rq) parameters investigated in the previous section, both surface roughness and topography are important parameters to consider when selecting implantable materials [38]. Furthermore, the evaluation of Sq parameter is paramount in the structural applications and initial stability of the dental implants during implantation.

3.1.3. Skewness parameters (Rsk and Ssk)

The performance of dental implants depends on the surface morphology and the material during their lifespan. Surface functionalisation on these materials depends upon the parameter used to characterise them. The surface roughness characterisation is an

Preprints (www.preprints.org) | NOT PEER-REVIEWED | Posted: 24 August 2021 doi:10.20944/preprints202108.0477.v1

important analytical method whereby one can understand the conditions of Ti-64 ELI [39]. The skewness was selected as one of the parameters to characterise the surface morphology of the samples. The results for 3.4 mm diameter 3D-printed dental implants Rsk show the lowest percentage of 0.595% compared to 1.102% for the 3D-printed dogbone tensile test specimens and 0.934% for the 4.3 mm diameter 3D-printed dental implants. The skewness parameter demonstrated a decrease in percentage when used in the samples with complex structures.

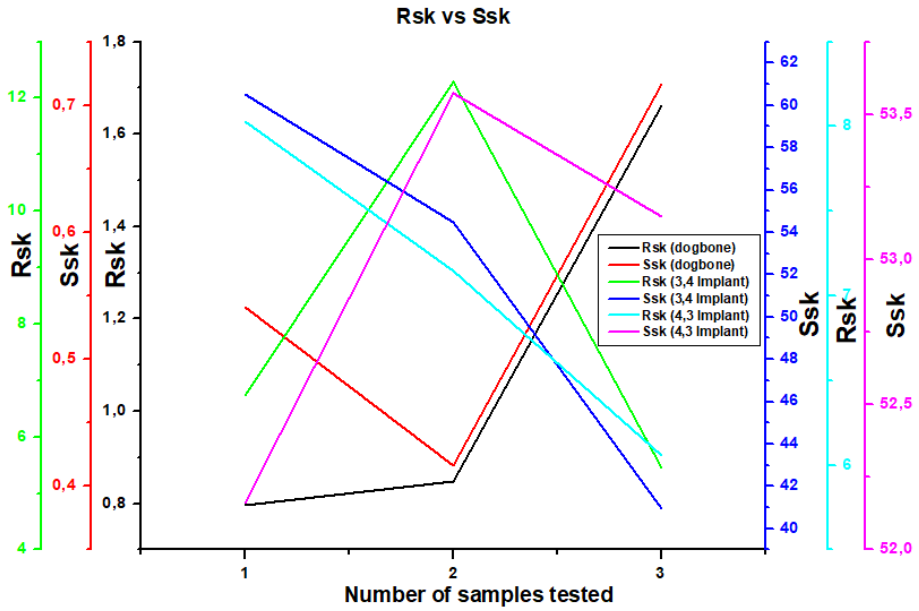

Figure 6: Graphical representation of 3D-printed specimen results with comparison of the skewness parameters (Rsk and Ssk) µm. 3D-printed dogbone tensile specimens, 3D-printed dental implant with a 3.4 mm diameter and 3D-printed dental implant with a 4.3 mm diameter are plotted against the number of specimens.

One of the greatest difficulties of additive manufacturing is the surface finish, and it might be difficult to use 3D-printed parts in other applications where surface finish is a critical factor [36]. An experimental study was carried out to enhance the surface finish of additively manufactured titanium samples through heat treatment [24]. Similarly, in the current study, heat treatment was performed on the 3D-printed samples to enhance the mechanical properties and improve surface roughness (see Figure 1). The findings can be explained as follows: The use of the skewness parameter is recommended for samples with a complex geometry, as it demonstrated minimum values of Rsk 0.596% and Ssk 0.169% (Figure 6).

3.1.4. Effect of heat treatment on tensile and fatigue properties

Table 6 shows the results of the tensile testing of 3D-printed specimens. The results are the average of each of the four specimens tested with standard deviations. Various 3D-printed specimens after fracture are shown in Figure 7. There was a visible change in the fracture point of the specimen. The tensile stress-strain graph is shown in Figure 8.

Preprints (www.preprints.org) | NOT PEER-REVIEWED | Posted: 24 August 2021 doi:10.20944/preprints202108.0477.v1

Table 6: Tensile test experimental result

	Maximum load [N]	**UTS [MPa]**	**Yield stress [MPa]**	**Tensile strain [mm/mm]**
1	7630.58	968.35	882.23	0.07
2	7527.35	955.25	853.97	0.08
3	7689.41	961.18	854.88	0.08
4	7581.17	947.65	846.60	0.08
Mean	7607.13	958.1	859.42	0.08
Std	69.18	8.79	15.64	0.0078

Figure 7: Fractured tensile test specimen

Preprints (www.preprints.org) | NOT PEER-REVIEWED | Posted: 24 August 2021 doi:10.20944/preprints202108.0477.v1

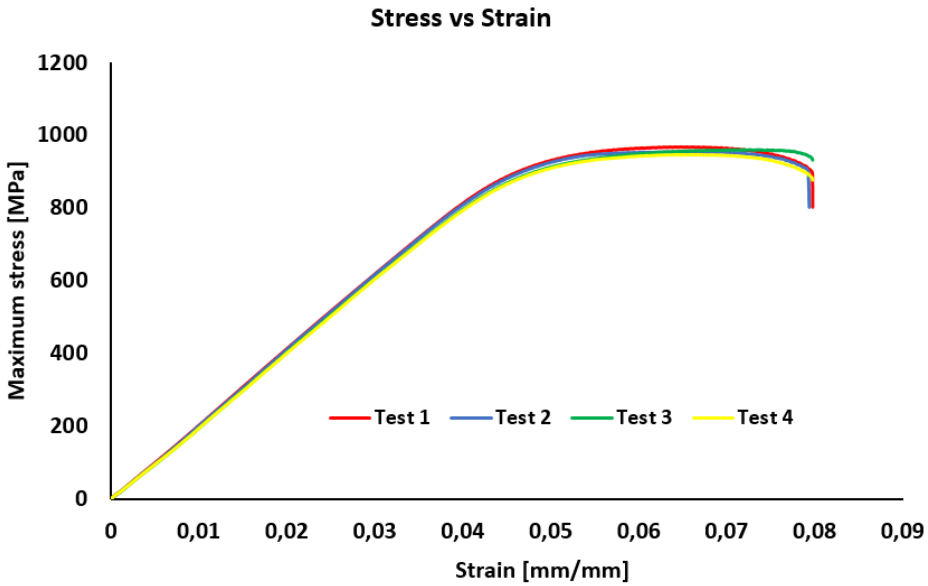

Figure 8: Stress vs strain graph

The first sample shows the highest yield strength of 882.22 MPa, while the lowest yield strength is Sample 4 at 846.60 MPa. Sample 1 was found to have the highest ultimate tensile strength of 968.35 MPa, which is consistent with the literature [8], [9], [24], [40]. Sample 3 was able to withstand a force of 7689.41N before breaking under tensile load. In the current research, samples fabricated by DMLS titanium (Ti-64 ELI) showed suitable mechanical properties – and are suitable for dental applications.

Table 6: Fatigue experimental results of 3.4 mm diameter dental implant

Samples	Cycles	Useful life [Years]
1	262 142	29.92
2	137 433	15.67
3	169 624	19.36
4	169 566	19.35
5	143 041	16.33
6	258 874	29.55
7	140 657	16.06
8	207 305	23.66
9	158 304	18.07
10	150 370	17.17

Preprints (www.preprints.org) | NOT PEER-REVIEWED | Posted: 24 August 2021 doi:10.20944/preprints202108.0477.v1

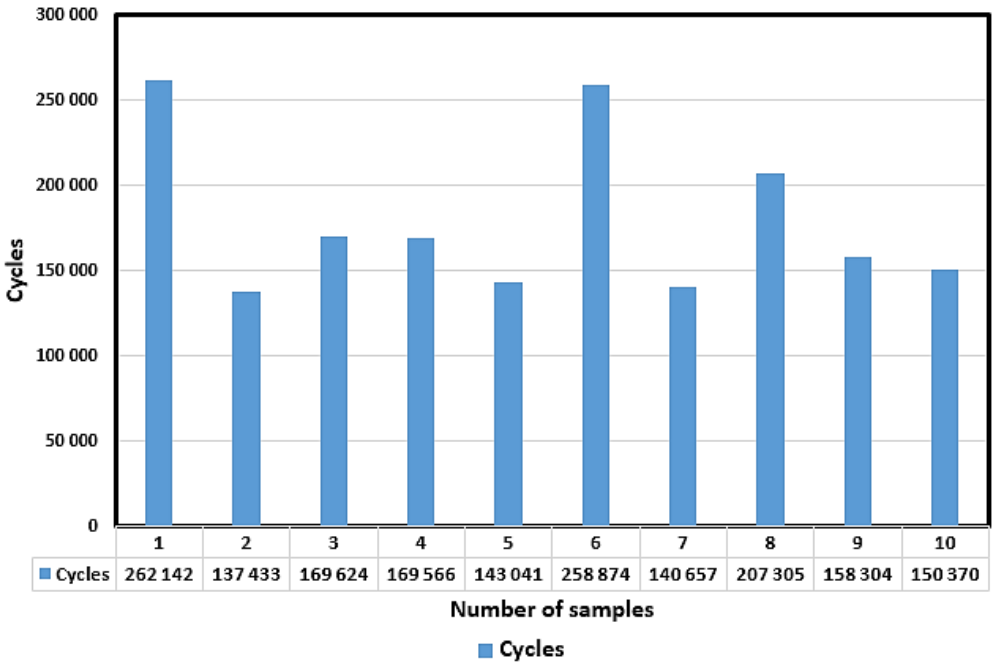

Figure 9: Fatigue experimental results of 3.4 mm

Table 6 shows 10 experimentally fractured 3.4 mm dental implants and reports the number of cycles and calculation of the service life. Figure 8 uses a bar chart to compare the number of completed cycles with the number of sample tests. The failure of the 3D-printed dental implant occurred in the second and third threads. The cycle target was set for 5×10^6 cycles but, with a loading of 80%, it was observed that a maximum of 262 142 and a minimum of 140 657 cycles respectively could be reached before failure occurred (see Figure 9). Sample 1 showed the longest life prediction, compared to Samples 2 to 10. The clinical success of 3D-printed dental implants has been seen at a maximum of 29.29 years and a minimum of 15.67 years when a masticatory load of 648.4N is applied.

3.1.5.Correlation between mechanical properties and the 3D-printed samples

This section describes the correlation of surface roughness and mechanical properties under the height parameter, amplitude parameter and skewness parameter. This was done to compare the mechanical properties of the tested samples with the surface roughness values obtained during surface roughness measurements.

Preprints (www.preprints.org) | NOT PEER-REVIEWED | Posted: 24 August 2021 doi:10.20944/preprints202108.0477.v1

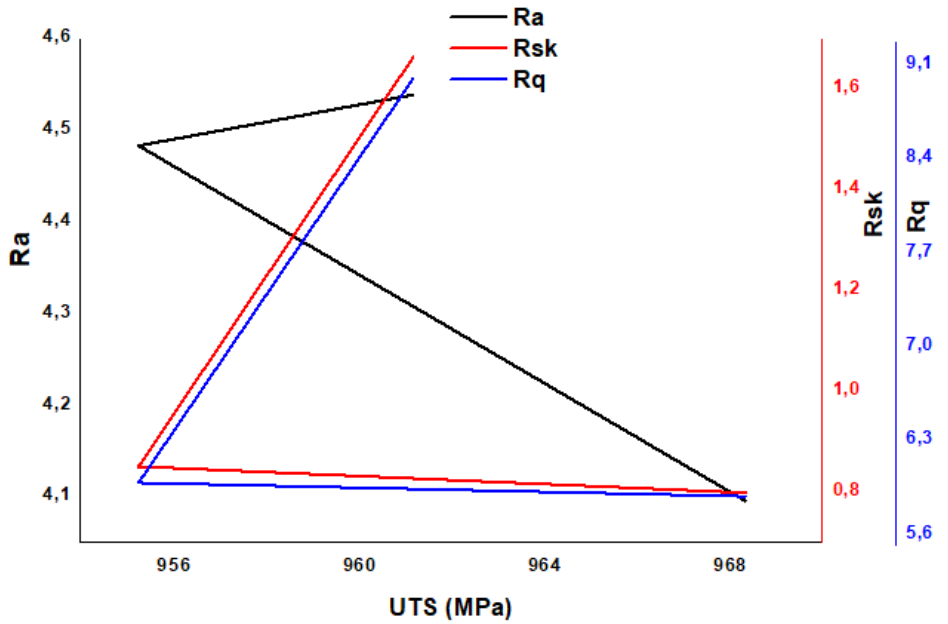

Figure 10: Comparison of surface roughness values against ultimate tensile stress (UTS MPa)

The results from Figure 10 show that Ra increases by 1.4% when ultimate tensile stress (UTS) decreases from 968.35 MPa to 955.25 MPa and by 0.6% when the UTS increases to 961.18 MPa. It was also noticed from the same figure that Rsk and Rq increase with the decrease in UTS. This surface roughness paramenters have a significant impact on the mechanical properties of 3D-printed samples under study.

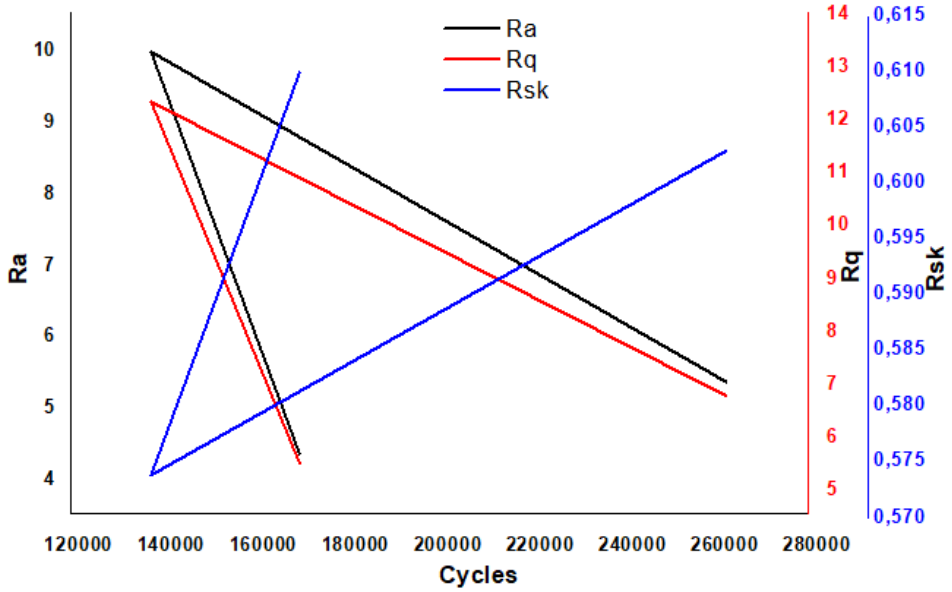

Figure 11: Comparison of fatigue experimental data against surface roughness

It was noticed from Figure 11 that when the cycles decrease by 137 433 from 262 142, the arithmetical mean height (Ra) for the 3D-printed dental implant also increases. In Figure 11, when the cycles decrease from 262 142 to 137 433, Ra increases by 90.74%, revealing

 doi:10.20944/preprints202108.0477.v1

lower cycle gain. It shows a 23% increase in Ra when the cycle increases from 137 433 to 169 624. In the same figure, it can be seen that Rsk and Rq also increase as the cycles decrease.

4. Conclusions

In the current study, the effects of surface roughness and mechanical properties of 3D-printed dental implants with diameters of 3.4 mm and 4.3 mm and 3D-printed dogbone tensile specimens were addressed. The outcomes of the study are:

- It was observed that crest and flank exhibited a smooth surface while the root had a rough surface for the 3D-printed dental implants, as shown in Figure 3. This could mean that between the threads, it was difficult for the 3D-printer to print a smooth surface due to the size and shape of the threads.
- It has been observed that samples with complex shapes show a higher roughness surface and pose the greatest difficulty in additive manufacturing when assessing the surface finish. In terms of surface roughness (Ra), the best results were obtained with a 3D-printed dogbone with an average of 4.371 μm, 4.3 mm 3D-printed dental with an average of 5.376 μm and 3.4 mm 3D-printed dental implant with an average 6.540 μm.
- Ra increases by 1.4% when the ultimate tensile stress (UTS) decreases to 955.25 MPa at 968.35 MPa and increases by 0.6% when the UTS increases to 961.18MPa. It can also be seen from Figure 10 that Rsk and Rq increase as UTS decreases.
- As a result of fatigue, when the cycles decrease from 262 142 to 137 433, Ra increased by 90.74% this huge difference adversely affects the fatigue properties of 3D-printed dental implants. Sample 1 showed the longest life prediction, compared to Samples 2 to 10 (see Figure 9).
- For 3D printed dental implants, the greater the surface roughness, the lower the mechanical properties, which in turn shortens the life of the implant and reduces its performance.

5. Limitation

The study is limited to a 3.4 mm diameter 3D-printed dental implant with 10 samples; the tensile test was performed on 4 samples and the heat treatment was done for 2 hours held at 800 ^{0}C.

List of abbreviations

DMLS = Direct metal laser sintered
EBM = Electron beam melting
ELI = Extra low interstitial Ra = Arithmetical mean height (μm)
Ra = Arithmetical mean height (μm)
Rsk = Skewness (μm)
Rq = Root mean square (μm)
Sa = Amplitude parameters (average of ordinates) (μm)
Ssk = Surface skewness (μm)

Sq = Root mean square roughness (μm)
stl = Standard translation language

Declarations

- **Acknowledgments**
  The research was supported by the Tshwane University of Technology and the University of South Africa (Unisa). The experiments were performed in biomechanics laboratory facilities at Unisa's Science Campus in Johannesburg, South Africa.
- **Availability of data and materials**
  The datasets used and/or analysed during the study are available from the corresponding author on reasonable request.
- **Competing interests**
  The author declares that he has no conflict of interest.
- **Funding**
  The project was funded through a Tshwane University of Technology scholarship and Unisa research funding.
- **Authors' contributions**
  Conceptualization, L.L.; methodology, L.L.; formal analysis, L.L,F.N. and D.D.; investigation, L.L, H.M, D.D. and F.N; resources, L.L. and H.N.; data curation, L.L and F.N.; writing—original draft preparation, F.N.; writing—review and editing, H.N. D.D. F.N and L.L.; visualization, F.N.; supervision, F.N, D.D and H.N.; project administration, L.L. and F.N.; funding acquisition, F.N. and H.N., All authors have read and agreed to the published version of the manuscript.

References

[1] A. Vaidya and K. Pathak, "Mechanical stability of dental materials," in *Applications of Nanocomposite Materials in Dentistry*, Woodhead Publishing, 2019, pp. 285–305.

[2] T. T. Oliveira and A. C. Reis, "Fabrication of dental implants by the additive manufacturing method : A systematic review," *J. Prosthet. Dent.*, pp. 1–5, 2019, doi: 10.1016/j.prosdent.2019.01.018.

[3] M. M. Ahsan, "3D Printing and Titanium Alloys : A Paper Review," *Eur. Acad. Res.*, vol. III, no. 10, pp. 11144–11154, 2016.

[4] C. Chang Tu, P. I. Tsai, S. Y. Chen, M. Y. P. Kuo, J. S. Sun, and J. Z. C. Chang, "3D laser-printed porous Ti6Al4V dental implants for compromised bone support," *J. Formos. Med. Assoc.*, vol. 119, no. 1P3, pp. 420–429, 2020.

[5] T. Becker, M. van Rooyen, and D. Dimitrov, "Heat treatment of TI-64L-4V produced by lasercuring," *South African J. Ind. Eng.*, vol. 26 (2), no. November 2014, pp. 93–103, 2015.

[6] B. Ren *et al.*, "Improved osseointegration of 3D printed Ti-6Al-4V implant with a hierarchical micro/nano surface topography: An in vitro and in vivo study," *Mater. Sci. Eng. C*, vol. 118, no. September 2020, p. 111505, 2021.

[7] M. D. Ashikur Rahman Khan and M. M. Rahman, "Surface finish characteristics of titanium alloy in a non conventional technique," in *International Conference on Recent Trends in Engineering and Material Sciences*, 2017, vol. 4, no. 9, pp. 9352–9355.

[8] D. J. Kuss, M. D. Griffiths, J. F. Binder, and B. Street, "Heat treatment of TI-6AL-4V produced by lasercusing," in *International RAPDASA conference*, 2015, vol. 26 (2), no. August 2015 V, pp. 93–103.

[9] M. G. Moletsane, P. Krakhmalev, N. Kazantseva, A. du Plessis, I. Yadroitsava, and I. Yadroitsev, "Tensile properties and microstructure of direct metal laser-sintered Ti6Al4V (ELI) alloy," *South African J. Ind. Eng.*, vol. 27, no. 3 Special Issue, pp. 110–121, 2016.

[10] T. Bhardwaj and M. Shukla, "Effect of laser scanning strategies on texture, physical and mechanical properties of laser sintered maraging steel," *Mater. Sci. Eng. A*, vol. 734, pp. 102–109, 2018.

[11] W. L. Xiao, H. B. Chen, and Y. Yin, "Effects of surface roughness on the fatigue life of alloy steel," *Key Eng. Mater.*, vol. 525–526, no. October 2015, pp. 417–420, 2012.

[12] B. Öztürk and F. Kara, "Calculation and Estimation of Surface Roughness and Energy Consumption in Milling of 6061 Alloy," *Adv. Mater. Sci. Eng.*, vol. 2020, 2020.

[13] G. Marenzi, F. Impero, F. Scherillo, J. C. Sammartino, A. Squillace, and G. Spagnuolo, "Effect of different surface treatments on titanium dental implant micro-morphology," *Materials (Basel).*, vol. 12, no. 5, 2019.

[14] A. Jemat, M. J. Ghazali, M. Razali, and Y. Otsuka, "Surface modifications and their effects on titanium dental implants," *Biomed Res. Int.*, vol. 2015, 2015.

[15] L. Le Guéhennec, A. Soueidan, P. Layrolle, and Y. Amouriq, "Surface treatments of titanium dental implants for rapid osseointegration," *Dent. Mater.*, vol. 23, no. 7, pp. 844–854, 2007.

[16] M. F. Kunrath, "Customized dental implants: Manufacturing processes, topography, osseointegration and future perspectives of 3D fabricated implants," *Bioprinting*, vol. 20, p. e00107, 2020.

[17] O. Obiukwu, N. Martin, B. Okafor, G. Lawa, and L. G. O.Obiukwu, M.Nwafor, B.Okafor, "The effect of surface finish on the low cycle fatigue of low and medium carbon steel'," *Int. Conf. Mech Ind. Engg*, no. August, 2015, [Online]. Available: https://www.researchgate.net/publication/335240807_The_Effect_of_Surface_Finish_on_the_Low_Cycle_Fatigue_of_Low_and_Medium_Carbon_Steel.

[18] A. Y. Suh, A. A. Polycarpou, and T. F. Conry, "Detailed surface roughness characterization of engineering surfaces undergoing tribological testing leading to scuffing," *Wear*, vol. 255, no. 1–6, pp. 556–568, 2003.

[19] M. Galati, P. Minetola, and G. Rizza, "Surface roughness characterisation and analysis of the Electron Beam Melting (EBM) process," *Materials (Basel).*, vol. 12, no. 13, 2019.

[20] S. Sneddon, Y. Xu, M. Dixon, D. Rugg, P. Li, and D. M. Mulvihill, "Sensitivity of material failure to surface roughness: a study on titanium alloys Ti64 and Ti407," *Mater. Des.*, vol. 200, p. 109438, 2020.

[21] A. Barman and M. Das, "Nano-finishing of bio-titanium alloy to generate different surface morphologies by changing magnetorheological polishing fluid compositions," *Precis. Eng.*, vol. 51, pp. 145–152, 2018.

[22] Z. Tang, F. Huang, and H. Peng, "Effect of 3D roughness characteristics on bonding behaviors between concrete substrate and asphalt overlay," *Constr. Build. Mater.*, vol. 270, p. 121386, 2021.

[23] B. Mooney and K. I. Kourousis, "A Review of of Maraging Factors Affecting Properties of Powder Bed Fusion," *Metals (Basel).*, vol. 10, no. 9, p. 1273, 2020.

[24] W. S. Gora *et al.*, "Enhancing surface finish of additively manufactured titanium and cobalt chrome elements using laser based finishing," *Phys. Procedia*, vol. 83, pp. 258–263, 2016.

[25] B. Godbey, "Surface Finish Control of 3D Printed Metal Tooling," Clemson University, 2007.

[26] P. Materials, E. I. Materials, P. Matrix, C. Materials, and P. Specimens, "Standard Test Method for Tensile Properties of Plastics 1," no. January 2004, pp. 1–15, 2006.

[27] A. T. Miller, "Fatigue and Cyclic Loading of 3D Printed Soft Polymers for Orthopedic Applications," no. May, p. 187, 2017.

[28] BSI Standards Publication dentistry, "BSI Standards Publication Dentistry — Implants — Dynamic loading test for

endosseous dental implants," 2016.

[29] A. Shaoki *et al.*, "Osseointegration of three-dimensional designed titanium implants manufactured by selective laser melting," *Biofabrication*, vol. 8, no. 4, pp. 1–10, 2016.

[30] C. Ma, Y. Dong, and C. Ye, "Improving Surface Finish of 3D-printed Metals by Ultrasonic Nanocrystal Surface Modification," *Procedia CIRP*, vol. 45, pp. 319–322, 2016.

[31] J. E. González *et al.*, "Influence of successive chemical and thermochemical treatments on surface features of Ti6Al4V samples manufactured by SLM," *Metals (Basel).*, vol. 11, no. 2, pp. 1–13, 2021, doi: 10.3390/met11020313.

[32] V. K. Wooding and R. F. Laubscher, "Variable length scale surface finish assessment of machined grade 4 titanium alloy," *Procedia CIRP*, vol. 13, pp. 90–96, 2014.

[33] A. Bernhardt *et al.*, "Surface conditioning of additively manufactured titanium implants and its influence on materials properties and in vitro biocompatibility," *Mater. Sci. Eng. C*, vol. 119, p. 111631, 2021.

[34] D. S. Ruppert, O. L. A. Harrysson, D. J. Marcellin-Little, S. Abumoussa, L. E. Dahners, and P. S. Weinhold, "Osseointegration of Coarse and Fine Textured Implants Manufactured by Electron Beam Melting and Direct Metal Laser Sintering," *3D Print. Addit. Manuf.*, vol. 4, no. 2, pp. 91–97, 2017.

[35] T. Kozior and J. Bochnia, "The influence of printing orientation on surface texture parameters in powder bed fusion technology with 316L steel," *Micromachines*, vol. 11, no. 7, 2020.

[36] A. Mostafaei, S. H. V. R. Neelapu, C. Kisailus, L. M. Nath, T. D. B. Jacobs, and M. Chmielus, "Characterizing surface finish and fatigue behavior in binder-jet 3D-printed nickel-based superalloy 625," *Addit. Manuf.*, vol. 24, pp. 200–209, 2018.

[37] A. Thakur, P. S. Rao, and M. Y. Khan, "Study and optimization of surface roughness parameter during electrical discharge machining of titanium alloy (Ti-6246)," *Mater. Today Proc.*, 2020.

[38] H. Zarei, M. Rosaria Marulli, M. Paggi, R. Pietrogrande, C. Üffing, and P. Weißgraeber, "Adherend surface roughness effect on the mechanical response of silicone-based adhesive joints," *Eng. Fract. Mech.*, vol. 240, no. September, 2020.

[39] M. Pacella, V. Nekouie, and A. Badiee, "Surface engineering of ultra-hard polycrystalline structures using a nanosecond Yb fibre laser: Effect of process parameters on microstructure, hardness and surface finish," *J. Mater. Process. Technol.*, vol. 266, no. June 2018, pp. 311–328, 2019.

[40] T. H. Becker, M. Beck, and C. Scheffer, "Microstructure and mechanical properties of direct metal laser sintered Ti-6Al-4V," *South African J. Ind. Eng.*, vol. 26, no. 1, pp. 1–10, 2015, doi: 10.7166/26-1-1022.